Determination of migration of ion-implanted Ar and Zn in silica by backscattering spectrometry

E. Szilágyi[a], I. Bányász[a], E. Kótai[a], A. Németh[a], C. Major[b], M. Fried[b] and G. Battistig[b]

[a]*Institute for Particle and Nuclear Physics, Wigner Research Centre for Physics, Budapest, Hungary*

[b]*Institute for Technical Physics and Materials Science, Centre for Energy Research, H-1121 Budapest, Konkoly Thege Miklós út 29-33, Hungary*

Corresponding author: E. Szilágyi

Institute for Particle and Nuclear Physics, Wigner Research Centre for Physics,

H-1121 Budapest, Konkoly Thege Miklós út 29-33, Hungary

E-mail: szilagyi.edit@wigner.mta.hu

Short biographical notes on all contributors.

Edit Szilágyi is the head of the Department of Materials Science by Nuclear Methods of the Wigner Research Centre for Physics. She graduated in physics at Kossuth Lajos University, Debrecen (1987), Ph. D. (Kossuth Lajos University, 1990), C.Sc. (1994) and D.Sc. (2011) of the Hungarian Academy of Sciences. Her work includes nuclear analysis using MeV energy ion beams (RBS - Rutherford Backscattering Spectrometry, ERDA - Elastic Recoil Detection Analysis, NRA - Nuclear Reaction Analysis, channelling). She developed a computer code to calculate the depth resolution of the above ion beam techniques. She has been extensively dealing with ion implantation and with fundamental processes of ion implantation in porous silicon, metals, and semiconductors.

István Bányász is a senior researcher at the Department of Materials Science by Nuclear Methods of the Wigner Research Centre for Physics. He received his Ph.D. in Physics from Loránd Eötvös University of Budapest, Hungary in 1987. He has worked in the fields of high-resolution holography, holographic non-destructive testing and holographic recording materials. His current research area is the application of ion- and electron beam irradiations to the

fabrication of optoelectronic components. Dr. Bányász is member of the Roland Eötvös Physical Society and Senior Member of SPIE - the International Society for Optics and Photonics.

Endre Kótai is senior research fellow of the Department of Materials Science by Nuclear Methods of the Wigner Research Centre for Physics. He graduated in physics at Loránd Eötvös University of Budapest. His main fields are Ion Beam Analysis (RBS, RBS/c, ERDA, NRA) and ion implantation. He developed computer codes to simulate, evaluate IBA spectra.

Attila Németh is senior research fellow of the Department of Materials Science by Nuclear Methods of the Wigner Research Centre for Physics. He graduated in physics at Uzhgorod State University (1994). From 1994 to 2003 he worked as research assistant in Institute of Electron Physics of National Academy of Scienses of Ukraine, Uzhgorod. In 2003 he obtained the title of candidate of physical-mathematical sciences in field of physics of electron-ion collisions and vacuum-ultraviolet spectroscopy (localized to Ph. D. in 2005). His present activities: development of ion sources, development, optimization and application of ion implantation techniques.

Csaba Major is currently working for the Department of Photonics in Res. Inst. for Technical Physics and Materials Science, Budapest, Hungary. Main research fields: Optical system designing, ellipsometer hardware development, evaluation of ellipsometric measurement.

Miklós Fried is currently the Head of Department of Photonics in Res. Inst. for Technical Physics and Materials Science, Budapest, Hungary. His main research field is: Investigation of surface modification of materials by ellipsometry and ion backscattering spectrometry.

Gábor Battistig, head of the Microtechnology Department, graduated in Electronic Technology in Faculty of Electrical Engineering, Technical University of Budapest (BME) in 1981. From 2006 he is the head of the Microtechnology laboratory of MFA. His research interests include various analytical methods for materials characterizations especially ion beam techniques. He is working in the development of Si based 3D MEMS devices as integrated gas, bio, chemical and mechanical sensors and the related processing technology with special emphasis on ion implantation and thin layer depositions.

Determination of migration of ion-implanted Ar and Zn in silica by backscattering spectrometry

It is well known, that the refractive indices of lots of materials can be modified by ion implantation, which is important for waveguide fabrication. In this work the effect of Ar and Zn ion implantation on silica layers was investigated by Rutherford Backscattering Spectrometry (RBS) and Spectroscopic Ellipsometry (SE). Silica layers produced by chemical vapour deposition technique on single crystal silicon wafers were implanted by Ar and Zn ions with a fluence of 1-2×10^{16} Ar/cm^2 and 2.5×10^{16} Zn/cm^2, respectively. The refractive indices of the implanted silica layers before and after annealing at 300 and 600 ^{o}C were determined by SE. The migration of the implanted element was studied by real-time RBS up to 500 ^{o}C. It was found that the implanted Ar escapes from the sample at 300 ^{o}C. Although the refractive indices of the Ar implanted silica layers were increased compared to the as-grown samples, but after the annealing this increase in the refractive indices is vanished. In case of the Zn implanted silica layer both the distribution of the Zn and the change in the refractive indices were found to be stable. Zn implantation seems to be an ideal choice for producing waveguides.

Keywords: waveguides, ion implantation, silica, chemical vapour deposition, Rutherford backscattering spectrometry, spectroscopic ellipsometry

Introduction

Optical waveguides have become basic elements of integrated optics and optoelectronics. Planar and channel waveguides are characterized by refractive indices. Several techniques are developed to set up and adjust refractive indices of optical materials (glasses, polymers, crystals, etc.). Further microelectronic technology can be used to fabricate integrated optics; therefore the thermal stability of waveguides is also important. Ion implantation, compared with other waveguide fabrication methods, has some unique advantages. It has proved to be a universal technique for producing waveguides in most optical materials. Moreover, ion implantation provides better

controllability and reproducibility in comparison with other techniques, e.g. diffusion of metal ions, ion exchange, sol gel and layer deposition techniques (for example sputtering, molecular beam epitaxy, and pulsed laser deposition, chemical vapour deposition). The first ion implanted waveguides were produced in 1968 by proton implantation into fused silica glass (*1*), and the changes in refractive indices due to H^+, He^+ and N^+ ion implantations have been characterized by several other groups (*2, 3, 4, 5*).

SiO_2 is an important insulating material with broad applications in the semiconductor and glass industries; therefore the thermal stability of the modified ion implanted layers is always an important question during device fabrication. In silica, the diffusion coefficient of several elements is higher compared to other materials (*6*); it is extremely high for example for He. Helium accumulation, migration and diffusion are intensively studied in nuclear materials because it has a strong influence on microstructural, physical and thermo-mechanical properties of natural or manufactured inorganic solids (*7, 8*). Because of the extremely high diffusion coefficient of the ion-implanted helium in silica, helium is able to escape from SiO_2 films, even from substoichiometric SiO_x films, if $x > 1.3$ (*9*). The helium can only be forced in silica, if buried silica island is formed (*10*), where the oxide is insulated properly from the vacuum.

The thermal stability of a layer, diffusion or migration of a given element can be studied by in-situ annealing combined with Rutherford Backscattering Spectrometry (RBS). The in-situ annealing/RBS technique is already mentioned in the proceedings of the 1st Ion Beam Conference (*11*), however, recently referred as real-time RBS is frequently used by several groups to study solid state reactions (*12, 13*).

In this work the effect of Ar and Zn ion implantation into CVD oxide layer were investigated in order to determine whether large enough increases in the refractive indices, suitable for waveguides applications, are produced. Ar is a noble gas similar to He, no chemical reaction with the target atoms occurs, while Zn more probably forms bonds with either Si or O. Mazzoldi and his co-workers published a comprehensive review on peculiarities and application perspectives of metal ion implantation in glasses in 1994 (*14*). They presented in detail experimental evidences of chemical interactions between the implanted metal ions and the target atoms, including Ti and W in pure SiO_2 and in silica glasses. Formation of nanometer-sized colloidal particles after implantation with metal ions was also demonstrated. Gao *et al.* reported synthesis of ZnS nanocrystallites in SiO_2 via multiple ion implantation and rapid thermal annealing (*15*). Amekura and his co-workers produced cupric oxide nanoparticles in silica glass by implantation of 60 keV Cu^- ions and subsequent thermal annealing in oxygen atmosphere (*16*). On basis of the above mentioned results, formation of layers with high concentration of ZnO nanoparticles (with a considerable refractive index change) in the SiO_2 thin layer could be expected.

Spectroscopic Ellipsometry (SE) and RBS were used to study the changes in refractive indices, and to determine the elemental composition of implanted films. Ar and Zn migration were followed by in-situ annealing/RBS technique. Since both Ar and Zn are heavier than the elements of the substrates, RBS is an ideal method to study their migration in the target material.

Experiment

In the present experiment first an oxide layer with a nominal thickness of 110 nm was formed on single crystal silicon (100) substrate by atmospheric pressure chemical

vapour deposition (CVD) technique. The deposition temperature was 450 ^{o}C. The whole wafer was cut to several pieces for implantation.

Two sets of three samples (each) were implanted by 50 keV Ar with a fluence of 1×10^{16} at/cm^2 or 2×10^{16} at/cm^2; two of them were implanted by 130 keV Zn ions with a fluence of 2.5×10^{16} at/cm^2. One of the Ar implanted samples was annealed for 1 h at 300 ^{o}C, while the other one at 600 ^{o}C. The third samples are referred as "as-implanted".

All the implanted and annealed samples as well as one of non-implanted samples were characterized by SE and RBS.

The optical properties and the thicknesses of thin film structures can be derived from (Ψ,Δ) values measured by SE, where Ψ and Δ describe the relative amplitude and relative phase change of polarized light during reflection, respectively. In the present experiment Ψ and Δ were measured by a Woollam M-2000DI rotating compensator ellipsometer in the 300 – 1700 nm wavelength range at angle of incidence of 70^{o} and 75^{o}. The refractive index of the layers was described by the Cauchy dispersion relation (*17*), an empirical polynomial approach for refractive index function of insulators and semiconductors below the band-gap (*18*). The calculated (generated) spectra were fitted to the measured ones using a regression algorithm. The measure of the fit quality is the mean square error (MSE) which was compared for different optical models. The unknown parameters are allowed to vary until the minimum of MSE is reached.

For standard RBS, the samples were fastened to a simple sample holder of a scattering chamber equipped with a two-axis goniometer. During the experiments the vacuum in the chamber was better than 1×10^{-4} Pa using liquid N_2 traps along the beam path and around the sample. The ion beam of 2000 keV $^4He^+$ was collimated with 2 sets of four-sector slits to the necessary dimensions of 0.5×0.5 mm^2. The ion current of typically 10 nA was kept constant via monitoring by a transmission Faraday cup (*19*).

The spectra were collected with a measurement dose of 4 μC. The RBS measurements were performed with an ORTEC surface barrier detector under a solid angle of 4.14 msr. The energy calibration of the multichannel analyser was performed by using known peaks and surface edges of Au, Si and C, respectively. To identify the surface elements and buried peaks, the RBS experiments were performed at least at two different tilt angles.

The hydrogen content of the as prepared oxide layer was determined by Elastic Recoil Detection Analysis (ERDA) using reflexion geometry at tilt 80^{o} and recoil angle of 20^{o} using 1600 keV He beam. The solid angle of the ERDA detector was 0.8 msr. To stop the forward scattered $^{4}He^{+}$ ions a Mylar foil of 6 μm thickness was applied before the ERD detector. To determine the hydrogen loss caused by the beam itself, 20 independent measurements were carried out with a dose of 0.2 μC each (therefore total dose was 4 μC).

To study the thermal stability of the layers in-situ annealing combined with RBS was carried out using a heated sample-holder. The temperature increased from room temperature (RT) to 500 ^{o}C with a linear ramping rate of 2.3 ^{o}C/min. In the case of Zn implanted sample 500 ^{o}C was kept for1 h. During the experiment RBS spectra were continuously collected with a dose of 1 μC using 2000 keV He^{+} beam. The collection time of a spectrum was about 40 s, i.e., hundreds of spectra were recorded. To improve the statistics several spectra can be summed during the evaluation, if it is necessary.

All the spectra taken on a sample were than simulated using the same layer structure obtained from the RBX simulation program (*20*).

Results and discussion

In the case of as prepared CVD oxide sample the elemental composition found to be

$SiO_{2.4}H_{0.16}$. The oxygen excess in the CVD oxide can be explained by oxygen excess-related defects (*21*). From the thicknesses given by ellipsometry (d_{SE}) and RBS (d_{RBS}, in at/cm^2 units) the density of the layer can be easily calculated as $\rho=d_{RBS}/d_{SE}$, resulting 6.18×10^{22} at/cm^3.

Ar implanted samples

The samples were implanted with two different Ar fluences. A maximum concentration of 0.87 at% and amount of ~8×10^{15} Ar/cm^2 has been found in the sample independently on the implanted fluences. RBS spectra of Ar implanted samples with fluences of 1×10^{16} at/cm^2 and 2×10^{16} at/cm^2 are shown in Fig. 1. Their depth distribution is far from the profile calculated by SRIM (*22*), Ar extends to the whole oxide layer. These results can be interpreted assuming limited number of traps for argon in the oxide matrix; if all the traps are occupied, the excess Ar can freely move in the layer and it can escape from the layer. Comparable results are found in similar fluence range for fused silica and soda-lime glass samples (*23*). These facts underline that this is an intrinsic property of silica, controlled by diffusion coefficients and the solubility limits, and it does not depend on the preparation methods.

Applying 1 h annealing in the implanted sample at 300 or 600 ^{o}C, all the Ar leaves the oxide layers. RBS shows that the composition and the layer thickness slightly changed, however, from these experiments we could not decide whether it is a real effect or only exhibits some inhomogeneity of the samples. As shown in Fig. 2, the refractive indices as a function of the incident wavelength determined by SE also show only small changes for the two different fluences. In case of the annealed samples, as the implanted ions escaped, the changes in the refractive indices are caused by only the structural modifications. The highest refractive indices were found for the case of the

as-implanted samples, then the refractive indices decrease as a function of temperature. After 600 °C annealing the refractive indices became lower than the as prepared sample. The densities of all Ar implanted oxide layer increase up to 6.6–6.8×10^{22} at/cm^3, that shows densification of the CVD oxide. These values are close to the density of thermal oxide (6.67×10^{22} at/cm^3).

Fig. 3 shows the results of in-situ annealing combined with RBS experiment performed on the sample implanted by low Ar fluence. The Ar peak area was determined as a function of the temperature. The uncertainty of the Ar peak areas was calculated on the basis of the uncertainty budget of the experiment (*24*). To increase the statistics, two successive spectra were summed. The Ar starts to escape at 225 °C, and there is another significant step at 350 °C. Finally, Fig. 4 presents the comparison of the spectra taken at RT and 450 °C, clearly showing the changes both in the composition and the layer thicknesses: not only the Ar escapes, but some oxygen loss is also occurred as the composition changed from $SiO_{2.3}Ar_{0.03}$ to $SiO_{2.1}$. The amount of silicon atoms in the oxide layer remains constant within experimental uncertainty.

Zn implanted samples

In case of Zn implanted sample the in-situ annealing/RBS measurement was carried out using the same linear ramping as it was used in the previous experiment. After reaching 500 °C, this temperature was kept for 1 h. The experiment proves that no change in the composition can be observed, as shown in Fig. 5.

The RBS profile shows that the Zn mainly stopped in the silica layer, but some particles reached the interface and stopped in the silicon. SE results can be interpreted, therefore, by a three-layer model. Two of them are the upper (low Zn-concentration) and the bottom (high Zn-concentration) part of the oxide layer with very different

behaviour of refractive indices as a function of wavelength, the third one is a thin partially amorphized layer on the substrate, next to the oxide. Only small changes in the refractive indices of oxide layer are observed due to 1h annealing at 500 ^{o}C, as shown in Fig. 6. Let us note that Cauchy dispersion relation is an empirical polynomial approach for refractive index function of insulators and semiconductors below the band-gap, so the reason of the different sign of dispersion below 500nm wavelength (see Fig. 6.c) is unknown. Maybe different phases (ZnO nanoparticles, mixed SiZnO phases) are involved. However, the wavelength region above 600 nm is the relevant region for the case of the waveguide applications. In spite of the fact that the implanted Zn ions entered into the Si substrate resulting partially amorphisation on the Si surface, the amplitude of the refractive index modulation across the SiO_2 layer reaches about 0.2 in the visible range. So fabrication of waveguide structures by this method seems to be feasible.

There are two significant differences between the Ar and Zn implanted samples: while Ar implantation changes the refractive indices of the whole layer, Zn modifies only a part of the layer. Moreover Zn implantation results much higher increase in the refractive indices than Ar implantation, and the increase is stable up to 500 ^{o}C.

Conclusions

The deposited CVD oxide was found to be not stoichiometric. A composition of $SiO_{2.4}H_{0.16}$ was measured with a lower density compared to the thermal oxide.

In case of the Ar implantation 0.87 at.% Ar is found in the oxide layer independently of the implanted fluence. Ar is not located near to the range expected from the SRIM calculation but extends to the whole oxide layer. The density of the layer increased. During 1 h ex-situ annealing at 300 ^{o}C, all the Ar leaves the layer.

Changes in refractive indices therefore can be interpreted by structural changes due to Ar implantation and annealing.

In-situ RBS results show that at least two Ar states exist in SiO_2, lower energy states and higher energy states release Ar at 225 ^oC and above 350 ^oC, respectively. The composition changed from $SiO_{2.4}Ar_{0.03}$ to $SiO_{2.1}$.

In case of Zn implantation no change in the composition can be observed during thermal annealing between RT and 500 ^oC. Ellipsometry results can be interpreted by three layer model. Two of them connected to the oxide layer with very different values of refractive indices as a function of wavelength, the third one is a thin partially amorphized Si layer on the substrate. Zn implantation causes much higher increase in the refractive indices than Ar implantation, and this increase is stable up to 500 ^oC. Therefore Zn implantation seems to be useful for waveguide applications.

Acknowledgement

The partial support of the Hungarian Scientific Research Fund (OTKA Grants No. K101223 and K112114) is acknowledged. Z. Zwickl is gratefully thanked for his technical help during the experiments.

References

(1) Schineller E.R.; Flam R.P.; Wilmot D.W. *J. Opt. Soc. Am.* **1968,** 58, 1171–1173.

(2) Townsend P.D.; Chandler P.J.; Zhang L *Optical effects of ion implantation;* Cambridge University Press: Cambridge, UK, **1994**.

(3) Peña-Rodríguez O.; Olivares J.; Carrascosa M.; García-Cabañes Á.; Rivera A.; Agulló-López F. (2012). Optical Waveguides Fabricated by Ion Implantation/Irradiation: A Review. In *Ion Implantation*, Goorsky M. Prof. Ed., ISBN: 978-953-51-0634-0, InTech, 2012; Chapter 12.

(4) Bányász I; Berneschi S.; Bettinelli M.; Brenci M.; Fried M.; Khanh N.Q.; Lohner T.; Nunzi Conti G.; Pelli S.; Petrik P.; Righini G.C.; Speghini A.; Watterich A.; Zolnai Z. *IEEE Photonics J.,* **2012,** 4, 721–727.

(5)Bányász I.; Zolnai Z.; Fried M.; Berneschi S.; Pelli S.; Nunzi Conti G. *Nucl. Instr. Meth. B,* **2014**, 326, 81–85.

(6) Francois-Saint-Cyr H.G.; Stevie F.A.; McKinley J.M.; Elshot K.; Chow L.; Richardson K.A. *J. Appl. Phys.* **2003,** 94, 7433–7439

(7) Trocellier P.; Miro S.; Serruys Y.; Vaubaillon S.; Pellegrino S.; Agarwal S.; Moll S.; Beck L. *Nucl. Instr: Meth. B* **2014,** 331, 55–64.

(8) P. Trocellier P.; Agarwal S.; Miro S. *J. Nucl. Mater.*, **2014***,* 445, 128–142.

(9) Manuaba A.; Pászti F.; Ramos A.R.; Khánh N.Q.; Pécz B.; Zolnai Z.; Tunyogi A.; Szilágyi E. *Nucl. Instr: Meth. B.* **2006***,* 249, 150–152.

(10) Szakács G.; Szilágyi E.; Pászti F.; Kótai E. *Nucl. Instr: Meth. B.* 2008, 266, 1382–1385.

(11) Baglin J.E.E.; Hammer W.N. in: Meyer O.; Linker G.; Käpeller F. (Eds.), Ion Beam Surface Layer Analysis, Plenum Press, New York, 1976, p. 447.

(12) Theron C.C.; Lombaard J.C.; Pretorius R. *Nucl. Instr: Meth. B.* **2000,** 161–163, 48–55.

(13) Demeulemeester J.; Smeets D.; Van Bockstael C.; Detavernier C.; Comrie C.M.; Barradas N.P.; Vieira A.; Vantomme A. *Appl. Phys. Lett.* **2008,** 93, 261912.

(14) Mazzoldi P. ; Arnold G.W. ; Battaglin G. ; Bertoncello D.; Gonella F. *Nucl. Instr: Meth. B.* **1994**, 91, 478–492.

(15) Gao K.Y.; Karl H.; Grosshans I.; Hipp W. ; Stritzker B. *Nucl. Instr: Meth. B.* **2002**, 196, 68–74.

(16) Amekura H.; Kono K; Takeda Y.; Kishimoto N. *Appl. Phys. Lett.* **2005**, 87, 153105.

(17) Langhoff P.; M. Karplus M. *J. Opt. Soc. Am.* **1969**, 59, 863–871

(18) Jenkins F.; White H. Fundamentals of Optics; (3rd ed.) McGraw-Hill, New York, 1957

(19) Pászti F.; Manuaba A.; Hajdu C.; Melo A.A.; da Silva M.F. *Nucl. Instr: Meth. B.* **1990,** 47 187–192.

(20) Kótai E. *Nucl. Instr: Meth. B.* **1994,** 85, 588–596.

(21) Skuja L.; Kajihara K.; Hirano M.; Hosono H. *Nucl. Instr: Meth. B.* **2012,** 286, 159–168.

(22)Ziegler J.F.; Ziegler M.D.; Biersack J.P. *Nucl. Instr. Meth. B*. **2010,** 268, 1818–1823

(23) Battaglin G.; Arnold G.W.; Mattei G.; Mazzoldi P.; Dran J.-C. *J. Appl. Phys.* **1999,** 85, 8040–8049.

(24) Jeynes C.; Barradas N.P.; Szilágyi E., *Anal. Chem.* **2012**, 84, 6061–6069.

Figures

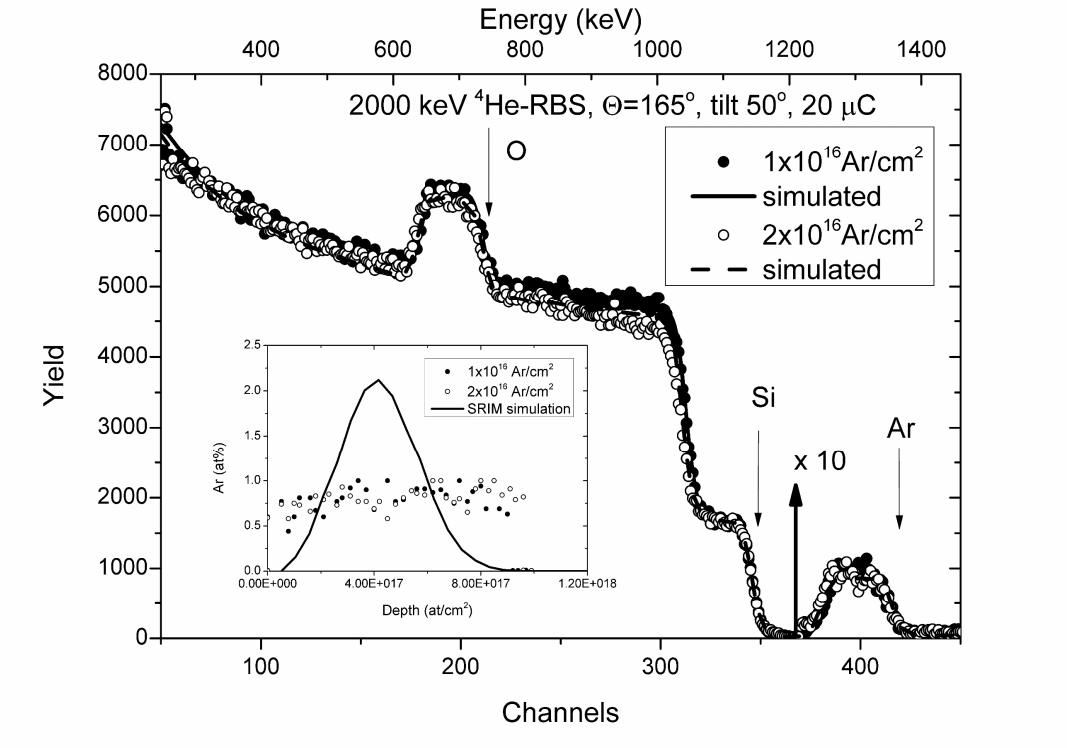

Figure1. RBS spectra taken on Ar implanted samples with fluence of 1×10^{16} at/cm^2 (L0) and 2×10^{16} at/cm^2 (H0). Inset shows the concentration profiles of Ar, and for the sake of the comparison the SRIM simulation is also shown that normalized the same amount of Ar.

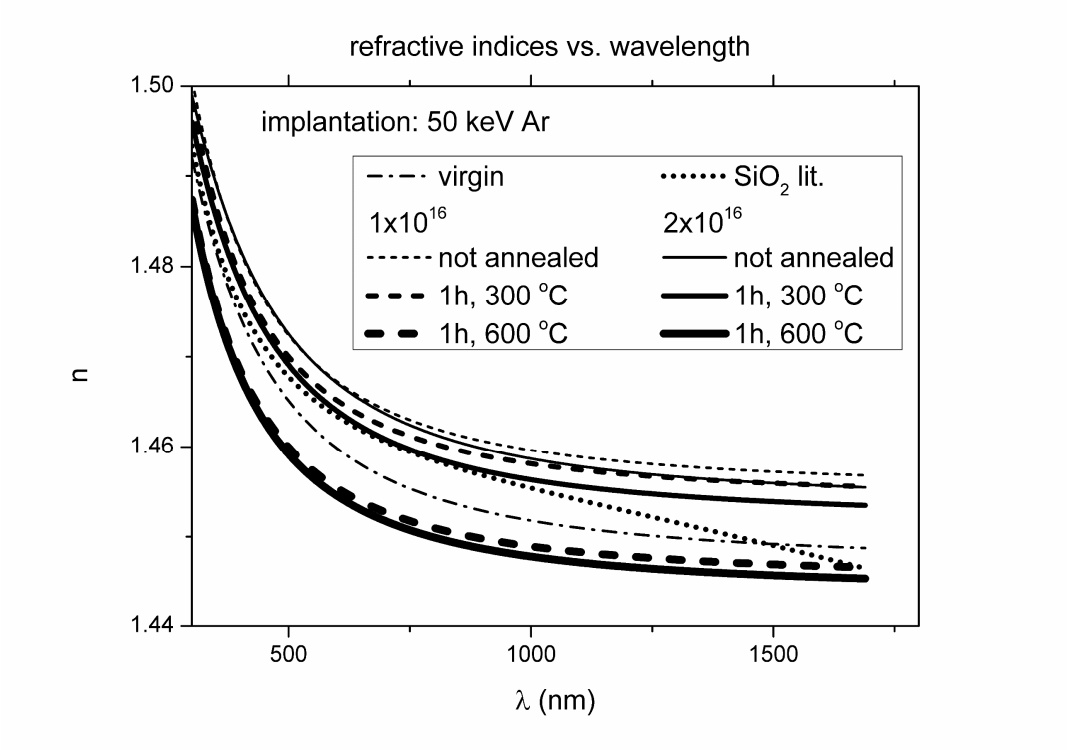

Figure 2. Refractive indices for Ar implanted samples. For comparison, the refractive indices of virgin sample and the thermal SiO_2 (from literature) are also shown.

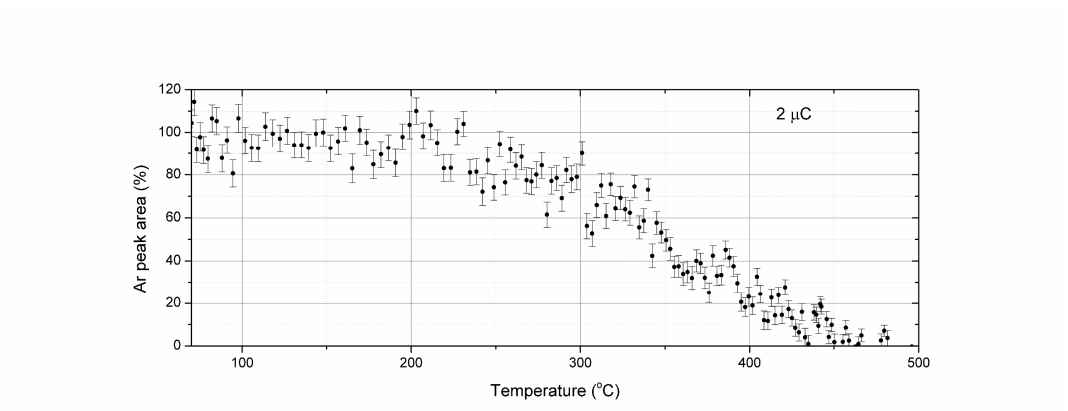

Figure 3. In-situ annealing combined with RBS experiment performed on the Ar implanted samples with fluence of 1×10^{16} at/cm^2.

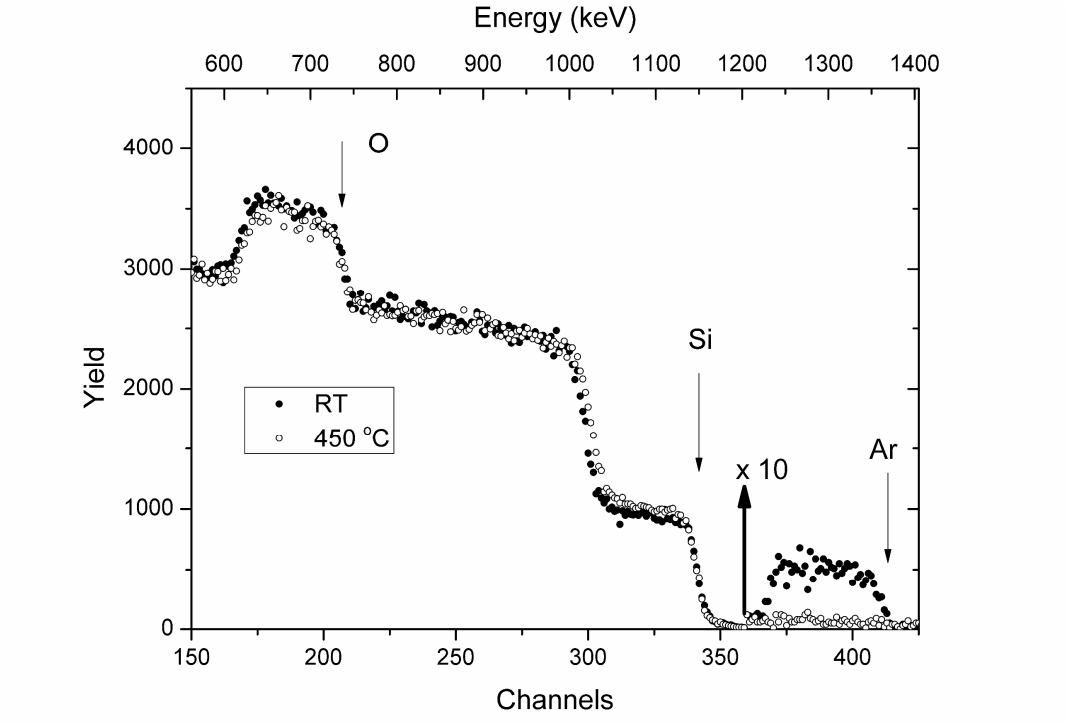

Figure 4. Composition changes. RBS spectra taken at RT and 450 °C during the in-situ annealing experiment. To increase the statistic 10 successive spectra were summed, that correspond to a dose of 10 μC.

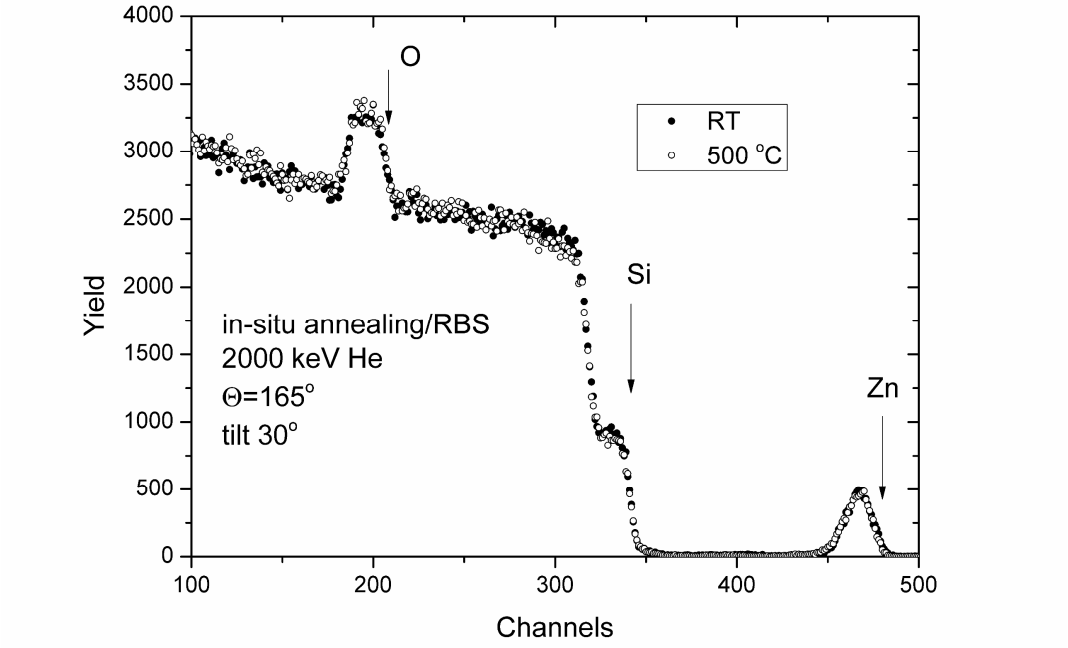

Figure 5. RBS spectra taken on Zn implanted sample at RT and 500 °C after 1 h annealing. Tilt was 30°; the dose of the spectra was 10 μC.

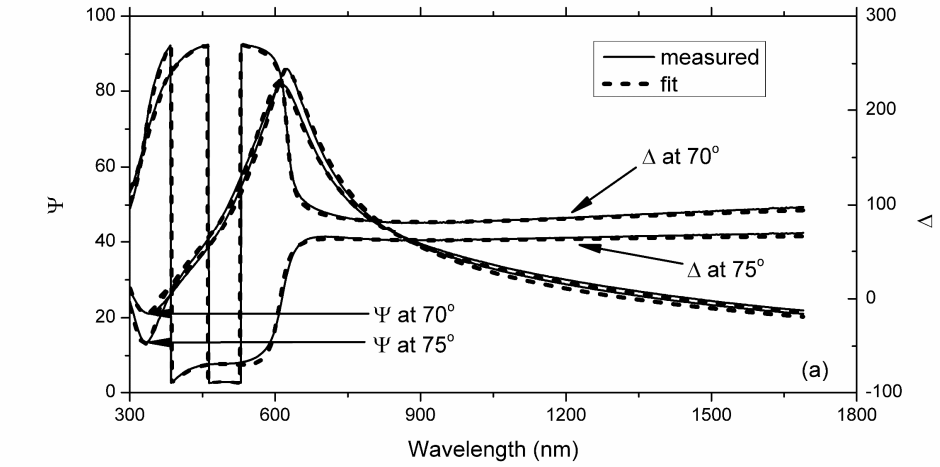
measured
fit
Δ at 70°
Δ at 75°
Ψ at 70°
Ψ at 75°
(a)
Ψ
Δ
Wavelength (nm)

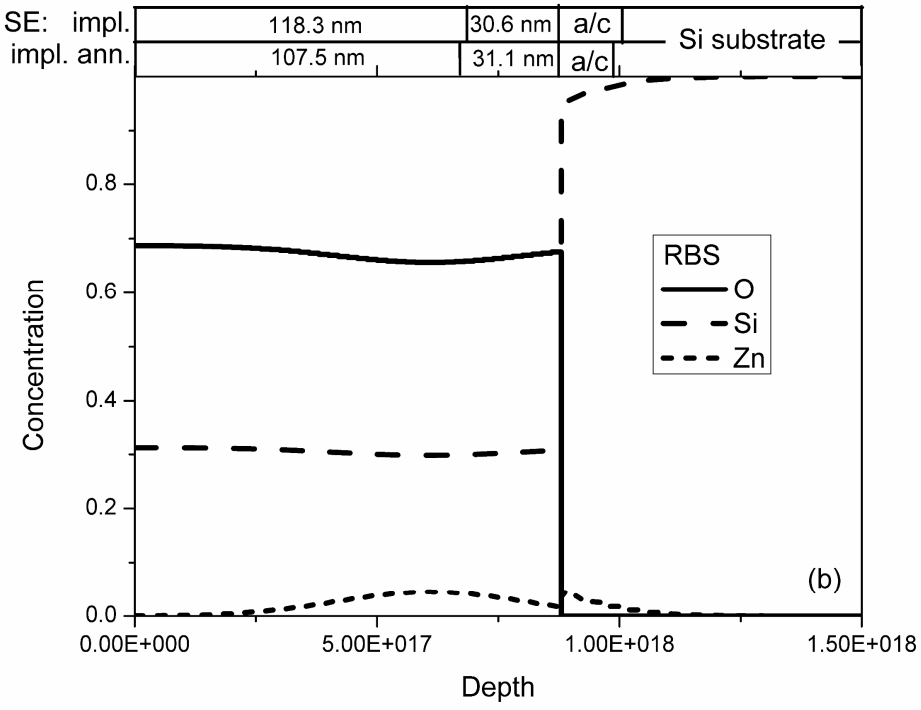
SE: impl.
impl. ann.
118.3 nm
30.6 nm
a/c
107.5 nm
31.1 nm
a/c
Si substrate
RBS
O
Si
Zn
(b)
Concentration
Depth

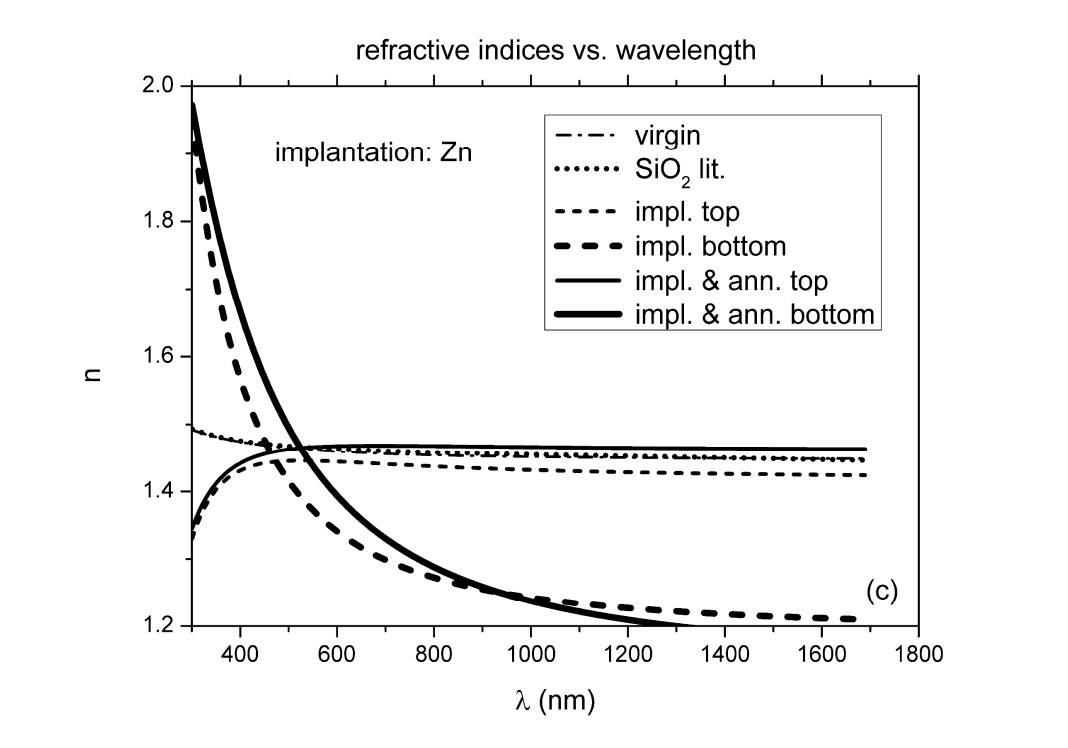

Figure 6. a) SE results on the Zn implanted sample after 1 h annealing at 500 °C. b) Comparison of depth profiles evaluated from RBS and SE. c) refractive indices as a function of wavelength for the two sublayers. For the sake of comparison the refractive indices of the virgin oxide as well as the thermal oxide are also shown.